Cell Metabolism
Article

Akt Stimulates Hepatic SREBP1c and Lipogenesis through Parallel mTORC1-Dependent and Independent Pathways

Jessica L. Yecies,[1] Hui H. Zhang,[1,3,5] Suchithra Menon,[1,5] Sihao Liu,[1] Derek Yecies,[1] Alex I. Lipovsky,[1,4] Cem Gorgun,[1] David J. Kwiatkowski,[2] Gökhan S. Hotamisligil,[1] Chih-Hao Lee,[1] and Brendan D. Manning[1,*]
[1]Department of Genetics and Complex Diseases, Harvard School of Public Health, Boston, MA 02115, USA
[2]Hematology Division, Department of Medicine, Brigham and Women's Hospital, Harvard Medical School, Boston MA 02115, USA
[3]Present address: Joslin Diabetes Center, Boston, MA 02115, USA
[4]Present address: Department of Genetics, Yale University School of Medicine, New Haven, CT 06520, USA
[5]These authors contributed equally to this work
*Correspondence: bmanning@hsph.harvard.edu
DOI 10.1016/j.cmet.2011.06.002

SUMMARY

Through unknown mechanisms, insulin activates the sterol regulatory element-binding protein (SREBP1c) transcription factor to promote hepatic lipogenesis. We find that this induction is dependent on the mammalian target of rapamycin (mTOR) complex 1 (mTORC1). To further define the role of mTORC1 in the regulation of SREBP1c in the liver, we generated mice with liver-specific deletion of TSC1 (*LTsc1KO*), which results in insulin-independent activation of mTORC1. Surprisingly, the *LTsc1KO* mice are protected from age- and diet-induced hepatic steatosis and display hepatocyte-intrinsic defects in SREBP1c activation and de novo lipogenesis. These phenotypes result from attenuation of Akt signaling driven by mTORC1-dependent insulin resistance. Therefore, mTORC1 activation is not sufficient to stimulate hepatic SREBP1c in the absence of Akt signaling, revealing the existence of an additional downstream pathway also required for this induction. We provide evidence that this mTORC1-independent pathway involves Akt-mediated suppression of *Insig2a*, a liver-specific transcript encoding the SREBP1c inhibitor INSIG2.

INTRODUCTION

The liver is a key organ in the systemic response to insulin, controlling both glucose and lipid metabolism. Hepatocytes respond to insulin by halting gluconeogenesis and increasing de novo lipid synthesis. Genetic mouse models have demonstrated that both of these responses to insulin occur, at least in part, downstream of the protein kinase Akt2 (Cho et al., 2001; Garofalo et al., 2003; Leavens et al., 2009). Akt2 mediates these effects primarily through the regulation of two downstream transcription factors, FOXO1 and SREBP1c, which control the expression of the metabolic enzymes underlying these processes (Figure S1A). FOXO1 stimulates gluconeogenic gene expression in the liver and is directly phosphorylated and inhibited by Akt (Gross et al., 2009). While the mechanisms are less well characterized, Akt signaling appears to stimulate de novo lipid synthesis through the activation of SREBP isoforms (reviewed in Krycer et al., 2010). SREBP1c is the dominant insulin-stimulated isoform in the liver, responsible for inducing lipogenic gene expression and promoting fatty acid synthesis (Horton et al., 2002). Akt activation appears to be both necessary and sufficient for the induction of hepatic SREBP1c and lipid accumulation (Fleischmann and Iynedjian, 2000; Leavens et al., 2009; Ono et al., 2003). An important feature of hepatic insulin signaling is that control of gluconeogenesis and lipogenesis is differentially affected under pathological conditions of insulin resistance associated with type 2 diabetes. Under such conditions, insulin fails to suppress glucose production by the liver, while the induction of hepatic lipogenesis is sustained, thereby contributing to both the hyperglycemic and hyperlipidemic states. Understanding this pathological phenomenon, referred to as selective insulin resistance (Brown and Goldstein, 2008), requires a deeper understanding of how insulin and Akt regulate hepatic lipid metabolism.

Recent cell-based studies have implicated the activation of mTOR complex 1 (mTORC1) downstream of Akt in the induction of SREBP isoforms (Düvel et al., 2010; Porstmann et al., 2008). The primary mechanism by which Akt activates mTORC1 is through the phosphorylation and inhibition of the TSC2 protein within the TSC1-TSC2 complex (reviewed in Huang and Manning, 2009). This protein complex acts as a GTPase-activating protein (GAP) for a Ras-related small G protein called Rheb, thereby enhancing its conversion to the GDP-bound off state. GTP-bound Rheb stimulates mTORC1 kinase activity and downstream signaling. Therefore, Akt-mediated inhibition of the TSC1-TSC2 complex serves to activate Rheb and mTORC1. Importantly, increased activation of mTORC1, through the expression of an activated allele of Akt (Porstmann et al., 2008) or genetic disruption of the TSC1-TSC2 complex (Düvel et al., 2010), has been found to activate SREBP isoforms and promote an SREBP-dependent increase in de novo lipid synthesis. Furthermore, a recent study has shown that the ability of insulin to stimulate SREBP1c in rat hepatocytes is sensitive to the mTORC1-specific inhibitor rapamycin (Li et al., 2010).

SREBP1c regulation is quite complex (Goldstein et al., 2006; Raghow et al., 2008). The protein is synthesized as an inactive

precursor that resides in complex with SREBP cleavage-activating protein (SCAP) in the endoplasmic reticulum (ER) membrane, where it is sequestered through the interaction of SCAP with INSIG proteins. Through a poorly understood process, insulin stimulates trafficking of the SREBP1c-SCAP complex to the Golgi, where SREBP1c is proteolytically processed to generate the active transcription factor. The active form of SREBP1c is sensitive to proteasomal degradation but can enter the nucleus to engage its transcriptional targets, including its own gene promoter and those encoding the major enzymes of fatty acid synthesis (Horton et al., 2002). A collection of previous studies has implicated insulin and Akt in controlling different aspects of SREBP1c activation (Krycer et al., 2010). While the mechanisms remain to be determined, mTORC1 signaling downstream of Akt appears to regulate some aspect of the trafficking or processing of SREBP isoforms, without obvious effects on translation or stability (Düvel et al., 2010; Porstmann et al., 2008).

The role of mTORC1 activation in the metabolic response of the liver to insulin and nutrients is poorly understood (Howell and Manning, 2011). Elevated levels of mTORC1 signaling have been associated with conditions of hepatic insulin resistance (Khamzina et al., 2005; Koketsu et al., 2008; Mordier and Iynedjian, 2007). In vitro, mTORC1 signaling can cause cell-intrinsic insulin resistance through negative feedback mechanisms affecting upstream regulators of Akt (Dibble et al., 2009; Harrington et al., 2005). In support of an in vivo role for these feedback mechanisms controlling insulin sensitivity, knockout of S6K1, a downstream target activated by mTORC1, leads to an increased response of Akt signaling to insulin in the mouse liver, as well as other metabolic tissues (Um et al., 2004). However, the phenotype of the S6K1 knockout mouse is confounded by a pronounced reduction in adiposity. Therefore, liver-specific genetic models are needed to better define the hepatocyte-intrinsic roles of mTORC1 in controlling insulin signaling and lipogenesis.

Here, we seek to elucidate the role of mTORC1 signaling in the regulation of SREBP1c and lipid metabolism in the liver. We find that mTORC1 activation is required for the induction of hepatic SREBP1c in response to insulin and feeding. To determine whether mTORC1 activation is sufficient to drive hepatic lipogenesis, we generate an mTORC1 gain-of-function mouse model lacking TSC1 in the liver. Contrary to our prediction, these mice are protected from both age- and diet-induced hepatic steatosis. In determining the mechanism of this protection, we find that there is a surprising defect in the induction of SREBP1c in the livers of these mice, stemming from the attenuation of hepatic Akt signaling. These findings indicate that mTORC1 activity alone cannot stimulate lipogenesis in the liver and that a second Akt-driven pathway is also required. Finally, our data indicate that the mTORC1-independent pathway downstream of Akt involves the suppression of a liver-specific isoform of INSIG (Yabe et al., 2003; Yellaturu et al., 2005, 2009).

RESULTS

Insulin Stimulates Hepatic SREBP1c in an mTORC1-Dependent Manner

As the mechanism of hepatic SREBP1c induction by insulin and Akt is poorly understood, we sought to determine whether mTORC1 activity contributes to this induction in primary mouse hepatocytes. Insulin stimulates activating phosphorylation events on Akt, leading to subsequent phosphorylation of the Akt targets FOXO1, FOXO3a, and TSC2, the latter target of which leads to mTORC1 activation and phosphorylation of S6K1 (Figures 1A and S1A). As described for other cell types, we find that inhibition of mTORC1 with rapamycin enhances the insulin-stimulated phosphorylation of Akt and its substrates in hepatocytes (Figure 1A), presumably through inhibition of negative feedback mechanisms (reviewed in Harrington et al., 2005; Huang and Manning, 2009). In response to insulin, SREBP1c induces its own expression, as well as genes encoding lipogenic enzymes, such as FASN (Horton et al., 2002; Raghow et al., 2008). Importantly, despite enhancing Akt signaling, pretreatment with rapamycin suppressed the ability of insulin to stimulate *Srebp1c* and *Fasn* (Figure 1B). In contrast, mRNA expression of *Igfbp1* and the gluconeogenic enzyme *Pepck*, two canonical FOXO1 targets, was inhibited by insulin but not affected by rapamycin (Figure S1B). These findings are consistent with those described recently for rat hepatocytes (Li et al., 2010) and demonstrate that mTORC1 is required for proper insulin stimulation of SREBP1c. Consistent with this effect on SREBP1c, rapamycin also significantly impairs the ability of insulin to stimulate de novo lipid synthesis in hepatocytes (Figure 1C). To determine the relevance of these findings in vivo, we subjected mice to an overnight fast, followed by refeeding. Feeding activates hepatic Akt and mTORC1 signaling and promotes the expression and processing of SREBP1 and increased expression of its targets (Figures 1D and 1E) (Horton et al., 1998). Importantly, SREBP1c activation was blocked by treatment with rapamycin just prior to feeding (Figures 1D and 1E), without effects on FOXO1 targets (Figure S1C). Taken together with studies in other settings (Düvel et al., 2010; Porstmann et al., 2008), these results indicate that mTORC1 is a critical effector downstream of insulin and Akt for the induction of SREBP1c in hepatocytes.

Liver-Specific Deletion of *Tsc1* Results in Insulin-Independent Activation of mTORC1

To further define the role of mTORC1 in the regulation of hepatic lipid metabolism, we employed a liver-specific gain of function model to disconnect mTORC1 activation from its normal control by insulin. As insulin signals to mTORC1 through Akt-mediated inhibition of the TSC1-TSC2 complex, loss of TSC1 or TSC2 leads to Akt-independent activation of mTORC1 signaling. To delete *Tsc1* specifically in hepatocytes, we used a previously described floxed allele of *Tsc1* (*Tsc1*^{fl}) (Figure 2A) (Kwiatkowski et al., 2002), backcrossed onto a pure C57BL/6J background. Following Cre-induced recombination, exons 17 and 18 of the *Tsc1*^{fl} allele are deleted, and this has been demonstrated to generate a null allele (Kwiatkowski et al., 2002). Hepatocyte-specific deletion of this allele was achieved by crossing these mice to those expressing Cre from the albumin promoter (*Alb-Cre*) (Postic and Magnuson, 2000). Genomic appearance of the null allele and liver-specific loss of TSC1 protein were confirmed by PCR genotyping (Figure 2B) and immunoblotting (Figure 2C), respectively, of liver extracts from littermates of different genotypes. Mice with homozygous loss of *Tsc1* in their livers (*Alb-Cre Tsc1*$^{fl/fl}$, referred to as *LTsc1KO*) were born at

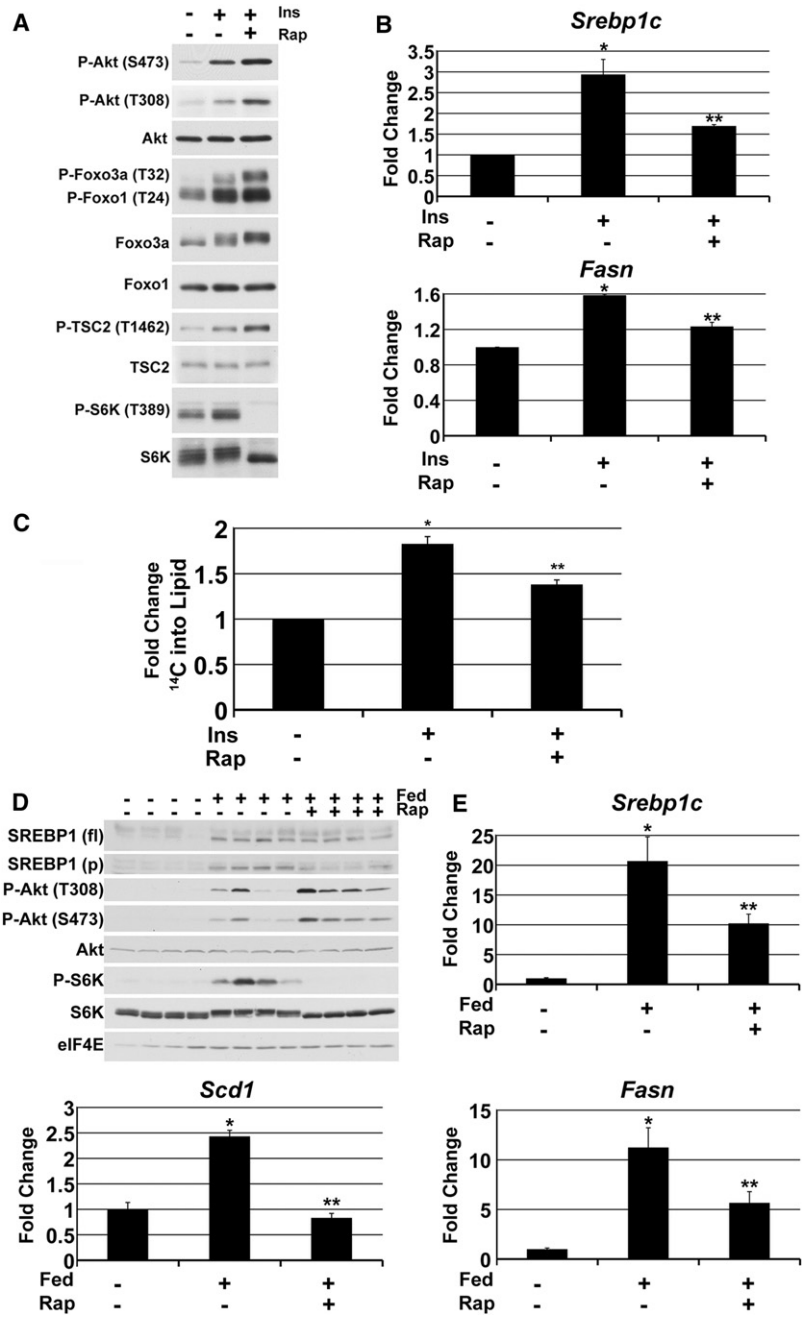

Figure 1. mTORC1 Activity Is Required for the Insulin-Stimulated Induction of Hepatic SREBP1c and De Novo Lipogenesis

(A) Primary hepatocytes were serum starved overnight, pretreated for 30 min with vehicle or rapamycin (Rap; 20 nM), and stimulated for 6 hr with insulin (Ins; 10 nM), as indicated.

(B) Hepatocytes were treated as in (A), and mRNA expression was measured by qRT-PCR. Transcript levels are shown relative to untreated controls. *$p < 0.006$ (*Srebp1c*) and $p < 4 \times 10^{-7}$ (*Fasn*) compared to unstimulated; **$p < 0.03$ (*Srebp1c*) and $p < 0.002$ (*Fasn*) compared to insulin-stimulated, vehicle-treated.

(C) Hepatocytes treated as in (A) were labeled with ^{14}C acetate, and the levels of ^{14}C incorporation into the lipid fraction are shown relative to untreated controls. *$p < 5 \times 10^{-5}$ and **$p < 0.004$ for the comparisons described in (B). Data are presented as the mean ± SEM from three (B) or four (C) independent experiments.

(D and E) Eight-week-old mice were fasted overnight (–) and then refed for 6 hr (+) following a 30 min pretreatment with vehicle or rapamycin (10 mg/kg). N = 4 mice per condition. Liver lysates were immunoblotted for markers of mTORC1 signaling and full-length (fl) and processed (p) SREBP1 (D). Gene expression was measured by qRT-PCR (E). Data are shown as mean ± SEM relative to untreated controls. *$p < 0.003$ (*Srebp1c*), $p < 0.002$ (*Fasn*), and $p < 0.0007$ (*Scd1*) compared to fasted; **$p < 0.03$ (*Srebp1c*), $p < 0.05$ (*Fasn*), and $p < 0.0001$ (*Scd1*) compared to fed, vehicle-treated.

Mendelian ratios and exhibited no loss of viability out to 9 months of age. As TSC1 stabilizes TSC2, *LTsc1KO* livers also exhibit a near-complete loss of TSC2 protein (Figure 2C). Importantly, only *LTsc1KO* livers exhibited increased phosphorylation of S6 and 4EBP1, reflected by decreased electrophoretic mobility, which are common readouts of mTORC1 signaling (Figures 2C and 2D). Hepatic mTORC1 signaling was sustained even under fasting conditions in the *LTsc1KO* mice, and the level of activation was comparable to control $Tsc1^{fl/fl}$ mice just after feeding (Figure 2E). Likewise, primary hepatocytes isolated from *LTsc1KO* mice exhibited insulin-independent activation of mTORC1 signaling (Figure 2F). Therefore, the *LTsc1KO* mice provide a model of hepatic mTORC1 activation that occurs independent of the upstream insulin-signaling pathway.

LTsc1KO Mice Are Protected from Age- and Diet-Induced Hepatic Steatosis

To begin to understand the role of mTORC1 signaling in the control of hepatic lipid metabolism, we examined the histological features of livers from cohorts of $Tsc1^{fl/fl}$ and *LTsc1KO* mice. Contrary to our expectations, *LTsc1KO* mice were protected from age-induced hepatic steatosis at 9 months, exhibiting significantly lower levels of liver triglycerides (TGs) (Figures S1A–S1C). A relative decrease in lipid accumulation in *LTsc1KO* livers was also evident in H&E-stained liver sections at 6 months (e.g., see Figure 2D). Given the surprising decrease in lipid accumulation in the livers of *LTsc1KO* mice fed a normal chow diet, we challenged the *LTsc1KO* mice with a lard-based high-fat diet (HFD) to further examine this phenotype. As on a chow diet (data not shown), there was no significant difference in weight gain between the $Tsc1^{fl/fl}$ and *LTsc1KO* mice on a HFD (Figure 3A). Dual-energy X-ray absorptiometry (DEXA) indicated that there was no difference in percentage body fat after 16 weeks of HFD (Figure 3B). However, the *LTsc1KO* mice exhibited protection from HFD-induced hepatic steatosis (Figure 3C). Blinded scoring of liver sections by a pathologist indicated that all $Tsc1^{fl/fl}$ mice had moderate to severe steatosis,

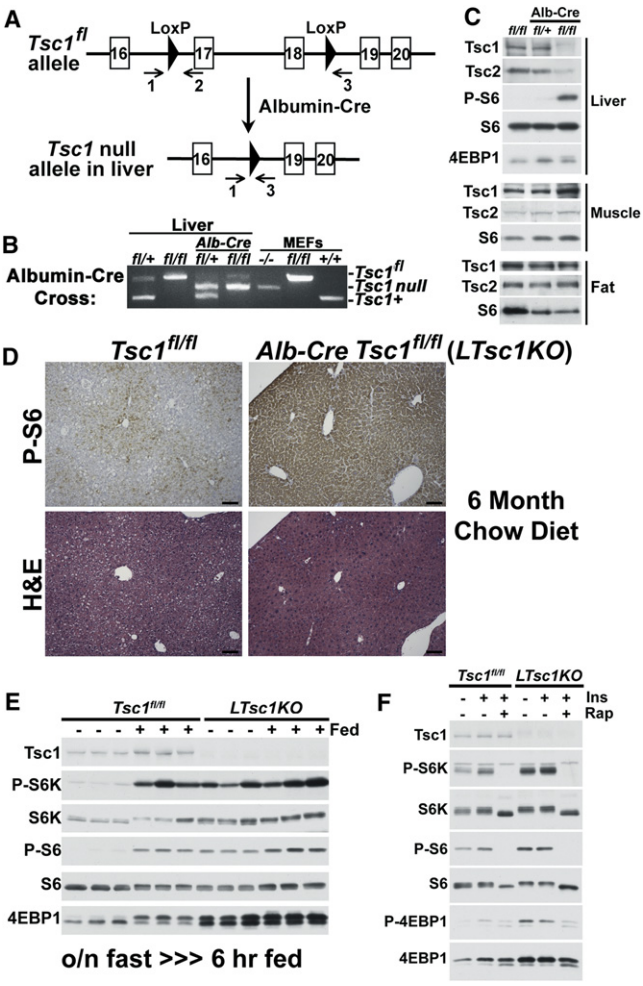

Figure 2. Liver-Specific *Tsc1* Deletion Renders Hepatic mTORC1 Signaling Constitutive and Insulin Independent

(A) Schematic of the *Tsc1*^{fl} allele and resulting null allele following Cre-mediated excision. The positions of the three PCR primers used for genotyping are shown with arrows.

(B) Representative PCR genotyping of liver tissue from the offspring of a cross between *Tsc1*$^{fl/fl}$ and *Albumin* (*Alb*)-*Cre* *Tsc1*$^{fl/+}$ mice using the primers shown in (A). Genomic DNA from MEFs of the given genotype was used as controls for the three *Tsc1* alleles.

(C) Immunoblots of liver, muscle, and fat tissue extracts from ad libitum-fed mice of the given genotypes are shown.

(D) Immunohistochemistry of phospho-S6 (S240/244) and staining with hematoxylin and eosin (H&E) were performed on adjacent liver sections from ad libitum-fed, 6-month-old mice of the given genotypes.

(E) Eight-week-old *Tsc1*$^{fl/fl}$ and *LTsc1KO* mice were fasted overnight (−) and then refed for 6 hr (+) where indicated (n = 3 mice per condition). Immunoblots of liver extracts from these mice are shown.

(F) Primary hepatocytes from *Tsc1*$^{fl/fl}$ and *LTsc1KO* mice were serum-starved overnight and stimulated for 6 hr with insulin (Ins; 10 nM) in the presence or absence of a 30 min pretreatment with rapamycin (Rap; 20 nM).

while the majority of *LTsc1KO* mice exhibited negative to mild lipid accumulation (Figure 3D). Consistent with these histological findings, *LTsc1KO* livers had significantly reduced levels of TGs (Figure 3E). Therefore, constitutive mTORC1 signaling in the *LTsc1KO* livers is accompanied by a decrease, rather than the predicted increase, in hepatic lipid accumulation.

LTsc1KO Mice Have Defects in Hepatic Induction of SREBP1c and Lipogenesis

To determine the mechanism of protection from hepatic steatosis in the *LTsc1KO* mice, we examined candidate pathways involved in lipid mobilization and metabolism. For instance, increased TG export could account for decreased accumulation in the liver. However, serum levels of TGs, nonesterified fatty acids (NEFAs), and cholesterol were not significantly different in mice fed a HFD, but TG and NEFA levels trended down in *LTsc1*KO compared to *Tsc1*$^{fl/fl}$ mice (Figure S2D). Furthermore, *LTsc1KO* mice did not display significant differences in hepatic TG output under fasting conditions, and again, these levels trended lower relative to controls (Figure S2E). Consistent with the lack of physiological evidence supporting a role for increased TG mobilization, transcript levels of proteins involved in these processes, such as *Mttp*, *Dgat1*, and *Dgat2*, were not significantly changed in *LTsc1KO* livers (Figure 3F). To address the possibility that *LTsc1KO* livers burn more lipid than controls, we measured expression of genes important for the β-oxidation of fatty acids. We found that transcript levels of *Pparα*, *Mcad*, and *Cpt1a* were not increased in the *LTsc1KO* livers, and in fact, *Mcad* expression was significantly reduced in these livers relative to controls (Figure 3G). This is consistent with recent findings that mTORC1 signaling decreases the expression of β-oxidation genes in the liver (Sengupta et al., 2010). As mitochondria are the major site of β-oxidation and mTORC1 signaling has been proposed to promote mitochondrial biogenesis (Cunningham et al., 2007), we also measured levels of mitochondrial markers. However, transcripts encoding the major mitochondrial transcription factor TFAM and the mitochondrial enzymes COX-IV and citrate synthase were not different (Figure S2F). Collectively, these results suggest that neither an increase in hepatic lipid output nor consumption underlies the protection from steatosis exhibited by the *LTsc1KO* mice.

Previous studies have demonstrated that mTORC1 signaling can drive lipogenesis through activation of SREBP isoforms (Düvel et al., 2010; Porstmann et al., 2008), and a similar role in the liver is supported by our findings above (Figure 1). However, like *LTsc1KO* mice, *Srebp1* knockout mice are protected from hepatic steatosis despite normal increases in adiposity (Yahagi et al., 2002). Therefore, we considered the possibility that *LTsc1KO* livers might have a defect in SREBP1c induction that could account for their decreased TG levels. Indeed, we found that the expression of *Srebp1c* and its lipogenic targets, *Fasn* and *Scd1*, were significantly reduced in the livers of *LTsc1KO* mice (Figure 4A). Consistent with a defect in SREBP1c activation, a more pronounced decrease in the levels of processed, active SREBP1 relative to full-length, inactive SREBP1 was detected in the *LTsc1KO* livers (Figure 4B). Reduced levels of FASN and SCD1 protein were also evident in these livers. The differences in lipogenic gene expression were not restricted to the HFD-fed group, but were also detected in young mice (8 weeks) fed a normal chow diet (Figure S3A). Furthermore, young *LTsc1KO* mice displayed defects in the hepatic induction of processed SREBP1 in response to feeding (Figure 4C). The decreased ratio of processed to full-length SREBP1 in the *LTsc1KO* livers is also reflected in decreased induction of its lipogenic targets at the protein and transcript levels (Figures 4C and 4D). *LTsc1KO* mice also exhibit defects in the feeding-induced

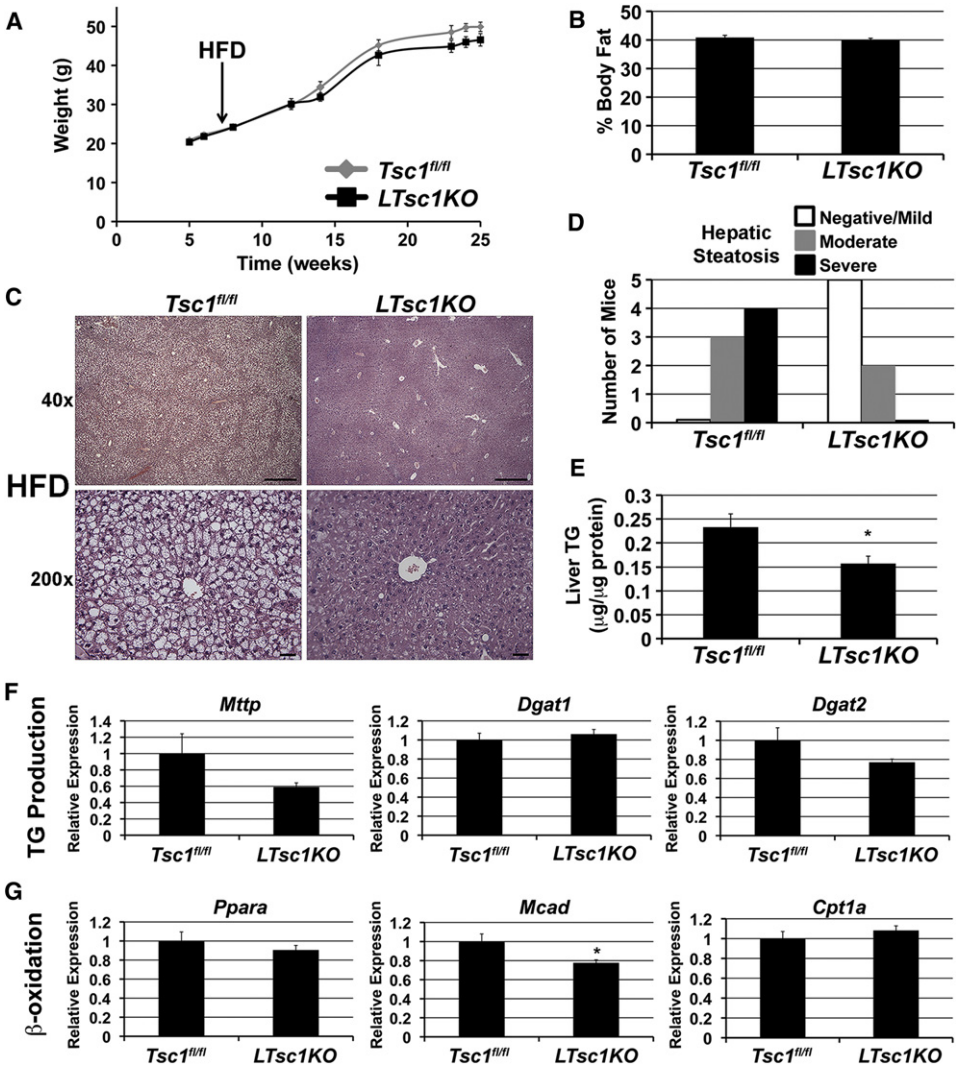

Figure 3. *LTsc1KO* Mice Are Protected from Diet-Induced Hepatic Steatosis

(A) A cohort of male *Tsc1*$^{fl/fl}$ (n = 3) and *LTsc1KO* (n = 4) mice were weighed between the ages of 5 and 25 weeks, while being fed a high-fat diet (HFD) for the final 16 weeks.

(B) HFD-fed male *Tsc1*$^{fl/fl}$ (n = 6) and *LTsc1KO* (n = 6) mice were subjected to DEXA scanning. In (A) and (B), data are presented as the mean ± SEM.

(C and D) Liver sections from 6-month-old *Tsc1*$^{fl/fl}$ (n = 7) and *LTsc1KO* (n = 7) mice fed a HFD, as in (A), were stained with H&E. Representative sections from these mice are shown (scale bars: 500 μm [40×], 50 μm [200×]) (C). The results from blinded scoring of the H&E-stained liver sections for negative/mild, moderate, or severe steatosis are provided (D).

(E) Liver triglycerides (TGs) were measured in ad libitum-fed *Tsc1*$^{fl/fl}$ (n = 5) and *LTsc1KO* (n = 5) mice on a HFD, as in (A). TG levels are shown normalized to protein concentration and are presented as the mean ± SEM. *$p < 0.05$.

(F and G) Expression of mRNA in the livers of ad libitum-fed *Tsc1*$^{fl/fl}$ (n = 4) and *LTsc1KO* (n = 4) mice on a HFD, as in (A), was measured by qRT-PCR for the given genes, and levels are presented as mean ± SEM relative to *Tsc1*$^{fl/fl}$. *$p < 0.05$ (*Mcad*).

expression of canonical SREBP2 target genes, including *Ldlr* and *Hmgcr* (Figure S3B) (Horton et al., 2002). Importantly, a hepatocyte-intrinsic defect in the induction of de novo lipid synthesis is detected in primary hepatocytes from *LTsc1KO* livers (Figure 4E), and there was a corresponding defect in the insulin-stimulated expression of *Srebp1c* and its target *Fasn* (Figure 4F). Taken together with our previous findings, these data indicate that mTORC1 activation is required but not sufficient to induce SREBP1c and lipogenesis in hepatocytes and suggest that defects in the induction of SREBP1c might underlie the protection of *LTsc1KO* mice from hepatic steatosis.

Elevated Hepatic mTORC1 Signaling Attenuates Insulin Signaling to Akt

Decreases in hepatic lipid accumulation and steatosis accompanied by decreases in SREBP1c and de novo lipogenesis are phenotypes described for the liver-specific knockout of Akt2 (Leavens et al., 2009). It has been well established in cell

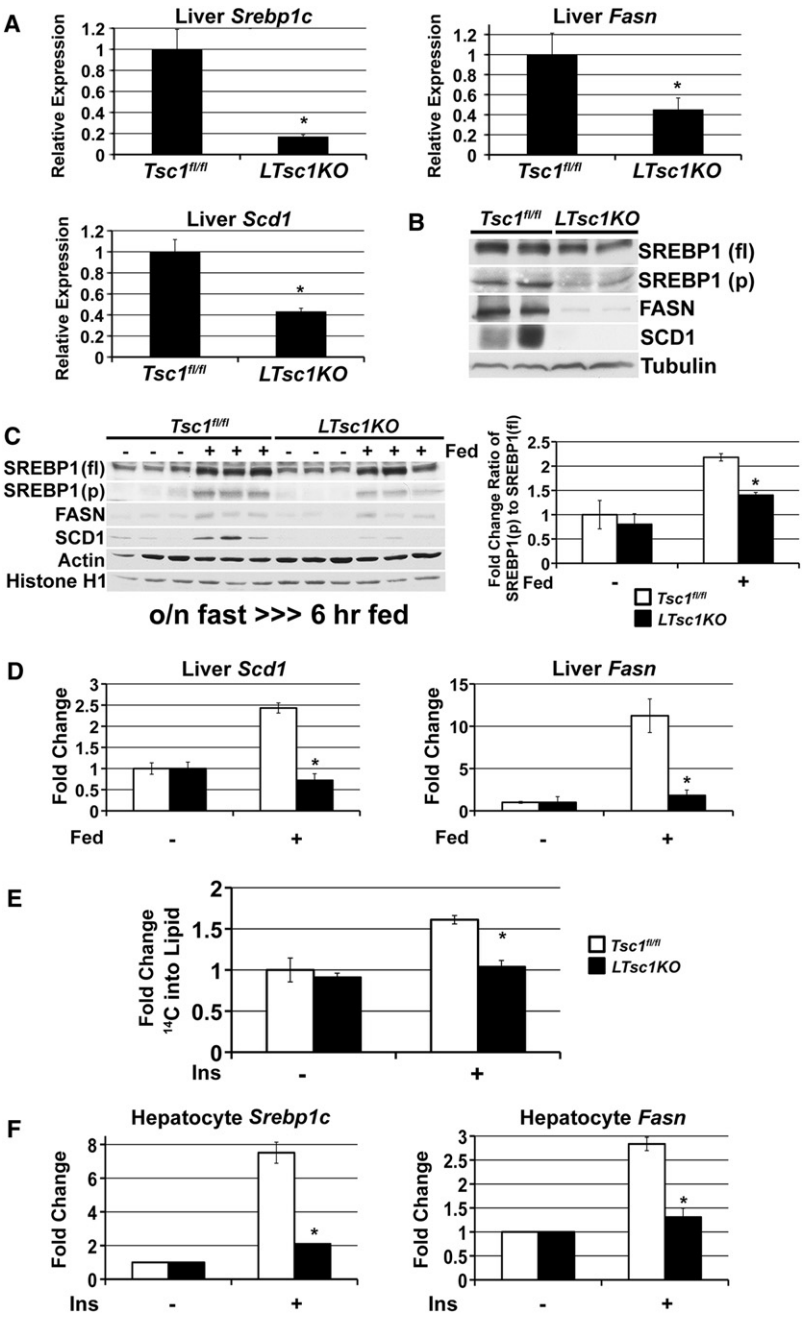

Figure 4. *LTsc1KO* Livers and Hepatocytes Have Defects in the Induction of SREBP1c Expression and De Novo Lipogenesis

(A) Expression of mRNA in the livers of male ad libitum-fed *Tsc1*$^{fl/fl}$ (n = 4) and *LTsc1KO* (n = 4) mice on a HFD was measured by qRT-PCR for the given genes, and levels are presented as mean ± SEM relative to *Tsc1*$^{fl/fl}$. *p < 0.005 (*Srebp1c*), p < 0.05 (*Fasn*), and p < 0.004 (*Scd1*).

(B) Immunoblots of full-length (fl) and processed (p) SREBP1, FASN, and SCD1 are shown in liver lysates from mice described in (A).

(C and D) Eight-week-old *Tsc1*$^{fl/fl}$ and *LTsc1KO* mice were fasted overnight (−) with or without refeeding for 6 hr (+) as indicated (n = 4 per condition). Liver lysates from *Tsc1*$^{fl/fl}$ and *LTsc1KO* mice were immunoblotted for full-length (fl) and processed (p) SREBP1 and its targets. The ratio of SREBP1(p) to SREBP1(fl) in the fasted and refed state was quantified for both genotypes and is presented as mean ± SEM relative to fasted wild-type samples. *p < 0.01 for the fold induction by feeding compared to *Tsc1*$^{fl/fl}$ livers (C). RNA was isolated from the livers of these mice, and gene expression was measured by qRT-PCR and is shown as mean ± SEM relative to fasted samples for each genotype. *p < 0.0005 (*Scd1*) and p < 0.003 (*Fasn*) for the fold induction by feeding compared to *Tsc1*$^{fl/fl}$ livers (D). Note: There are no significant differences in fasted expression levels between *Tsc1*$^{fl/fl}$ and *LTsc1KO* livers.

(E) Primary hepatocytes from *Tsc1*$^{fl/fl}$ and *LTsc1KO* mice were serum starved overnight, followed by insulin stimulation (Ins; 10 nM) for 6 hr. Cells were labeled with ^{14}C acetate for the final 4 hr, and its incorporation into the lipid fraction was measured. Data are presented as the mean of duplicate samples ± SEM relative to unstimulated wild-type samples. *p < 0.01 for the fold induction by insulin compared to *Tsc1*$^{fl/fl}$ hepatocytes.

(F) Expression of mRNA from primary hepatocytes treated as described in (E) was analyzed by qRT-PCR for the given genes, and levels are presented as the mean of duplicate samples ± SEM relative to the unstimulated samples for each genotype. *p < 0.013 (*Srebp1c*) and p < 0.023 (*Fasn*) for the fold induction by insulin compared to *Tsc1*$^{fl/fl}$ hepatocytes. Data in (E) and (F) are representative of at least three independent experiments.

culture models that mTORC1 activation stimulates negative feedback mechanisms that can dampen the response of cells to insulin, resulting in decreased Akt signaling (reviewed in Harrington et al., 2005; Huang and Manning, 2009). However, it is unknown whether mTORC1 activation in the liver can cause hepatic insulin resistance. Indeed, *LTsc1KO* mice display decreased phosphorylation of Akt and its downstream target FOXO1 in their livers (Figure 5A). In contrast, phosphorylation of GSK3α and β was not substantially different in *Tsc1*$^{fl/fl}$ and *LTsc1KO* livers, consistent with the fact that additional protein kinases can phosphorylate these Akt substrates (Cross et al., 1995; Eldar-Finkelman et al., 1995; Fang et al., 2002; Zhang et al., 2006). Atypical PKCs have also been implicated in the promotion of hepatic lipogenesis downstream of the insulin receptor (Matsumoto et al., 2003; Taniguchi et al., 2006). However, the activating phosphorylation of PKCζ/λ was increased, rather than decreased, in the *LTsc1KO* livers (Figure S4A), perhaps suggesting a compensatory mechanism. As the AMP-dependent protein kinase (AMPK) has recently been found to block the processing of SREBP isoforms (Li et al., 2011), we also examined AMPK activation, but found no difference between the control and *LTsc1KO* livers (Figure S4B). One feedback mechanism by which mTORC1 activation is thought to inhibit insulin signaling is through the downregulation of IRS1 protein levels (reviewed in Harrington et al., 2005), and indeed, IRS1 levels were reduced in *LTsc1KO* livers (Figure 5A). As would be expected from the defect in Akt-mediated phosphorylation of FOXO1, *LTsc1KO* mice

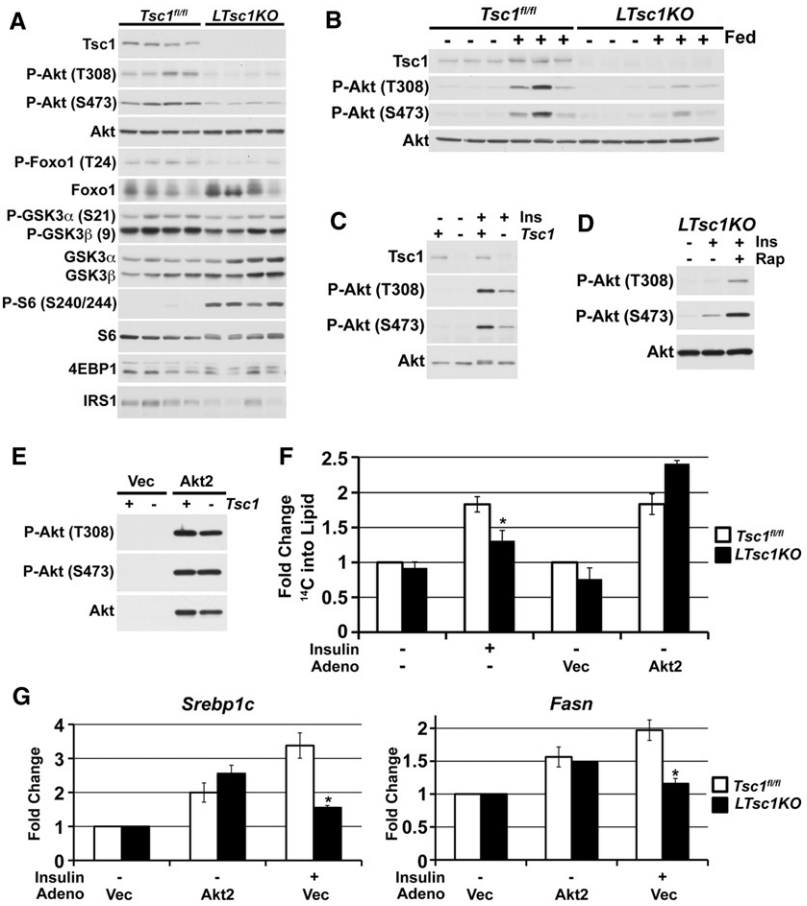

Figure 5. Attenuation of Akt Signaling in *LTsc1KO* Livers and Hepatocytes Is Responsible for the Defect in SREBP1c Induction

(A) Immunoblots of liver lysates from ad libitum-fed male *Tsc1*$^{fl/fl}$ and *LTsc1KO* mice following a 16 week HFD are shown for the indicated phospho- (P) and total proteins.

(B) Eight-week-old *Tsc1*$^{fl/fl}$ and *LTsc1KO* mice were fasted overnight (–) with or without refeeding for 6 hr (+) as indicated prior to immunoblot analysis of liver lysates.

(C) Primary hepatocytes from *Tsc1*$^{fl/fl}$ (+) and *LTsc1KO* (–) mice were serum starved overnight and then stimulated with insulin (Ins; 10 nM) for 1 hr where indicated.

(D) Following overnight serum starvation, *LTsc1KO* hepatocytes were treated with rapamycin (Rap; 20 nM) for 30 min where indicated prior to insulin stimulation (10 nM) for 6 hr.

(E) Primary hepatocytes from *Tsc1*$^{fl/fl}$ and *LTsc1KO* mice were infected with adenovirus expressing either empty vector (Vec) or myr-Akt2 (Akt2), and 6 hr postinfection, cells were serum starved overnight before lysis and immunoblotting.

(F) Following overnight serum starvation, uninfected cells were stimulated with insulin (10 nM) for 6 hr, whereas cells infected as in (E) were left unstimulated. Cells were labeled with ^{14}C acetate for the final 4 hr, and its incorporation into the lipid fraction was measured. Data are presented as the mean of duplicate samples ± SEM relative to unstimulated *Tsc1*$^{fl/fl}$ samples for the uninfected group or to the vector-expressing *Tsc1*$^{fl/fl}$ samples for the infected group and are representative of at least two independent experiments. *$p < 0.05$ for the difference in fold induction by insulin compared to *Tsc1*$^{fl/fl}$ hepatocytes.

(G) Primary hepatocytes were infected as described in (E), with vector-expressing cells being treated with insulin (10 nM) for 6 hr where indicated. Expression of mRNA was measured by qRT-PCR for the given genes, and levels are presented as mean ± SEM relative to the unstimulated vector-expressing group for each genotype ($n = 3$). *$p < 0.027$ (*Srebp1c*) and $p < 0.024$ (*Fasn*) for the fold induction by insulin compared to *Tsc1*$^{fl/fl}$ hepatocytes.

exhibit a significant increase in hepatic expression of the FOXO1 targets *Pepck* and *Igfbp1* (Figure S4C) and a decrease in glucose tolerance (Figure S4D) relative to controls. However, *LTsc1KO* mice do not display differences in insulin tolerance (Figure S4E). Young *LTsc1KO* mice on a normal chow diet also exhibit attenuation of Akt activation in response to feeding (Figure 5B). Finally, a cell-intrinsic reduction in the ability of insulin to stimulate Akt was confirmed in primary hepatocytes from *LTsc1KO* livers (Figure 5C), and this was rescued by pretreatment with rapamycin (Figure 5D). The hepatocyte-intrinsic defect in insulin sensitivity in *LTsc1KO* mice is further supported by the fact that there are no significant differences in circulating insulin levels on either a normal chow or high-fat diet (Figure S4F). Therefore, uncontrolled mTORC1 activity in the liver causes defects in insulin signaling to Akt.

Restoration of Akt Signaling to *LTsc1KO* Hepatocytes Rescues SREBP1c Induction

To determine whether the mTORC1-dependent attenuation of Akt signaling underlies the defect in the ability of insulin to stimulate lipogenesis in *LTsc1KO* hepatocytes, we employed a membrane-targeted constitutively active allele of Akt2 (myr-Akt2), which bypasses negative-feedback mechanisms acting on upstream components in the pathway. Unlike endogenous Akt (Figure 5C), adenovirally delivered myr-Akt2 is phosphorylated to a similar extent in both *Tsc1*$^{fl/fl}$ and *LTsc1KO* hepatocytes (Figure 5E). Interestingly, restoring Akt2 signaling to *LTsc1KO* hepatocytes ameliorated their defect in lipogenesis. Unlike insulin, myr-Akt2 stimulated similar levels of de novo lipid synthesis in both *Tsc1*$^{fl/fl}$ and *LTsc1KO* hepatocytes (Figure 5F). As expected from this rescue of lipogenesis, and in contrast to insulin, myr-Akt2 also induced expression of *Srebp1c* and *Fasn* to a similar extent in *Tsc1*$^{fl/fl}$ and *LTsc1KO* hepatocytes (Figure 5G). These findings support a model in which Akt2 signaling is essential for the induction of hepatic SREBP1c and lipogenesis and that, in addition to a requirement for mTORC1 activity, at least one additional parallel pathway downstream of Akt2 is essential for this induction.

INSIG2a Suppression Is an mTORC1-Independent Mechanism Regulating SREBP1c Downstream of Akt

To gain insight into the mTORC1-independent mechanism of SREBP1c induction downstream of Akt2, we examined the regulation of candidate pathways. Akt and other kinases

phosphorylate and inhibit GSK3α and β, which have been found to regulate the stability of processed, active SREBP isoforms in cell culture models (Sundqvist et al., 2005). However, unlike Akt and FOXO1, we did not observe substantial differences in the inhibitory phosphorylation of GSK3 in the livers or hepatocytes of *LTsc1KO* mice (Figures 5A and S5A). Another potential candidate for SREBP1c regulation downstream of Akt is the LXR family of nuclear receptors, which can transcriptionally activate *Srebp1c* in response to insulin (Hegarty et al., 2005). However, no significant differences in the expression of *Lxra* or *Lxrb* or their canonical transcriptional target *Abca1* were detected in the *LTsc1KO* livers (Figure S5B).

Unlike hepatocytes, mTORC1 signaling is both necessary and sufficient to activate SREBP isoforms in other cell types (Düvel et al., 2010; Porstmann et al., 2008). Therefore, we decided to investigate a mechanism of SREBP1c regulation that is believed to be specific to the liver. Insulin signaling has been found to suppress a liver-specific transcript encoding the SREBP-inhibitory protein INSIG2, called *Insig2a* (Yabe et al., 2003; Yellaturu et al., 2005, 2009). As INSIG proteins can block the induction of hepatic SREBP1c and lipogenesis (Engelking et al., 2004, 2005; Takaishi et al., 2004), the suppression of *Insig2a* is likely to contribute to the activation of SREBP1c in response to insulin (Yabe et al., 2003). Interestingly, we found that *LTsc1KO* livers express elevated levels of *Insig2a* transcripts and INSIG2 protein (Figures 6A and S5C). This is in contrast to *Insig1*, which is a known transcriptional target of SREBP and, like other targets, is reduced in the *LTsc1KO* livers (Figures S5C and S5D). Consistent with the insulin-stimulated suppression of *Insig2a* functioning in a parallel pathway to mTORC1, we found that rapamycin does not affect *Insig2a* suppression in intact livers or isolated hepatocytes from wild-type mice (Figures 6B and 6C). However, an Akt-specific inhibitor (Aktviii) completely reversed the suppression of *Insig2a* in response to feeding or insulin, indicating that this mechanism occurs downstream of Akt. The feeding-induced suppression of INSIG2 protein levels was blocked in a dose-dependent manner by the Akt inhibitor (Figure S5E). In contrast to the differential effects on *Insig2a* expression, the Akt inhibitor and rapamycin have similar inhibitory effects on the induction of SREBP1c processing and expression (Figures S5F, 6B, and 6C). Consistent with the elevated expression of *Insig2a* in *LTsc1KO* livers (Figure 6A), *LTsc1KO* hepatocytes are defective in the suppression of *Insig2a* in response to insulin (Figure 6D). Importantly, the restoration of Akt signaling to *LTsc1KO* hepatocytes completely rescues the suppression of *Insig2a* (Figure 6D). Consistent with Akt-mediated downregulation of *Insig2a* being required for proper *Srebp1c* induction, forced expression of *Insig2* significantly decreased the ability of activated Akt to stimulate *Srebp1c*, while having no effect on its suppression of the FOXO1 target *Igfbp1* (Figure S5G). Finally, siRNA-mediated suppression of *Insig2a* in *LTsc1KO* hepatocytes restores the insulin-stimulated induction of *Srebp1c* (Figure 6E), while maintaining the defect in insulin-mediated suppression of *Pepck* (Figure S5H). Collectively, these data are consistent with two parallel pathways downstream of Akt2, one involving the suppression of *Insig2a* expression and the other requiring mTORC1 activation, both being essential for insulin-stimulated induction of hepatic SREBP1c (Figure 6F).

DISCUSSION

Recent genetic evidence suggests that Akt is a major effector of insulin signaling for the induction of hepatic lipogenesis (Fleischmann and Iynedjian, 2000; Leavens et al., 2009; Ono et al., 2003). Whole-body and liver-specific knockouts of Akt2 are protected from hepatic steatosis under conditions of obesity caused by leptin deficiency (*ob/ob*) or a lard-based HFD (Leavens et al., 2009). This phenotype is similar to that described for *Srebp1* knockout mice, which are also protected from steatosis in the background of obesity (Yahagi et al., 2002). Importantly, the protection from hepatic lipid accumulation in the Akt2 knockout models is accompanied by reduced expression of *Srebp1c* and decreased de novo lipogenesis, suggesting that a defect in SREBP1c induction underlies this phenotype. However, on a coconut oil-based HFD with sucrose (Surwit), the liver-specific Akt2 knockout mice do not exhibit defects in the expression of *Srebp1c* or its lipogenic targets but maintain their reduced levels of hepatic TGs. This suggests that SREBP1c-independent pathways downstream of Akt might also contribute to hepatic lipid content. Interestingly, mice with liver-specific deletion of *Pten*, which exhibit constitutive activation of Akt signaling, develop severe hepatic steatosis on a normal chow diet (He et al., 2010; Stiles et al., 2004), and this phenotype is dependent on Akt2 and its regulation of lipogenic gene expression downstream of SREBP1c (He et al., 2010). Likewise, hepatic expression of constitutively active Akt also induces SREBP1c and causes fatty liver disease and hypertriglyceridemia (Ono et al., 2003), much like transgenic overexpression of SREBP1c itself (Shimano et al., 1997). While studies have indicated that atypical PKCs might play a parallel role (Matsumoto et al., 2003; Taniguchi et al., 2006), these collective findings demonstrate that Akt is a major insulin-responsive effector in the induction of hepatic SREBP1c. While this regulation appears to contribute to both physiological and pathological hepatic lipid accumulation, the critical mechanisms downstream of Akt are not well defined.

Together with a recent study in rats (Li et al., 2010), our current findings indicate that mTORC1 is an essential downstream target of insulin and Akt signaling for the proper induction of SREBP1c and lipogenesis in the liver. However, the *LTsc1KO* mouse model demonstrates that mTORC1 activation alone is not sufficient to induce SREBP1c. We were particularly surprised to find that chronic mTORC1 signaling, instead, leads to a decrease in the induction of SREBP1c and lipogenesis and protection from both age- and diet-induced hepatic steatosis. The decreased activation of SREBP1c in *LTsc1KO* hepatocytes is the result of mTORC1-driven inhibitory feedback mechanisms causing insulin resistance and attenuation of Akt signaling to its other downstream pathways. Due to the disconnect between Akt and mTORC1 signaling in these mice, the *LTsc1KO* model affords a unique experimental system in which to identify mTORC1-independent pathways and processes downstream of Akt in the liver. Analyses of the *LTsc1KO* mice revealed that Akt stimulates hepatic SREBP1c and lipogenesis through parallel mTORC1-dependent and independent pathways and that the latter pathway involves suppression of a liver-specific inhibitor of SREBP1c.

Although functionally similar, distinct mechanisms regulate the expression and stability of INSIG1 and INSIG2 (Goldstein

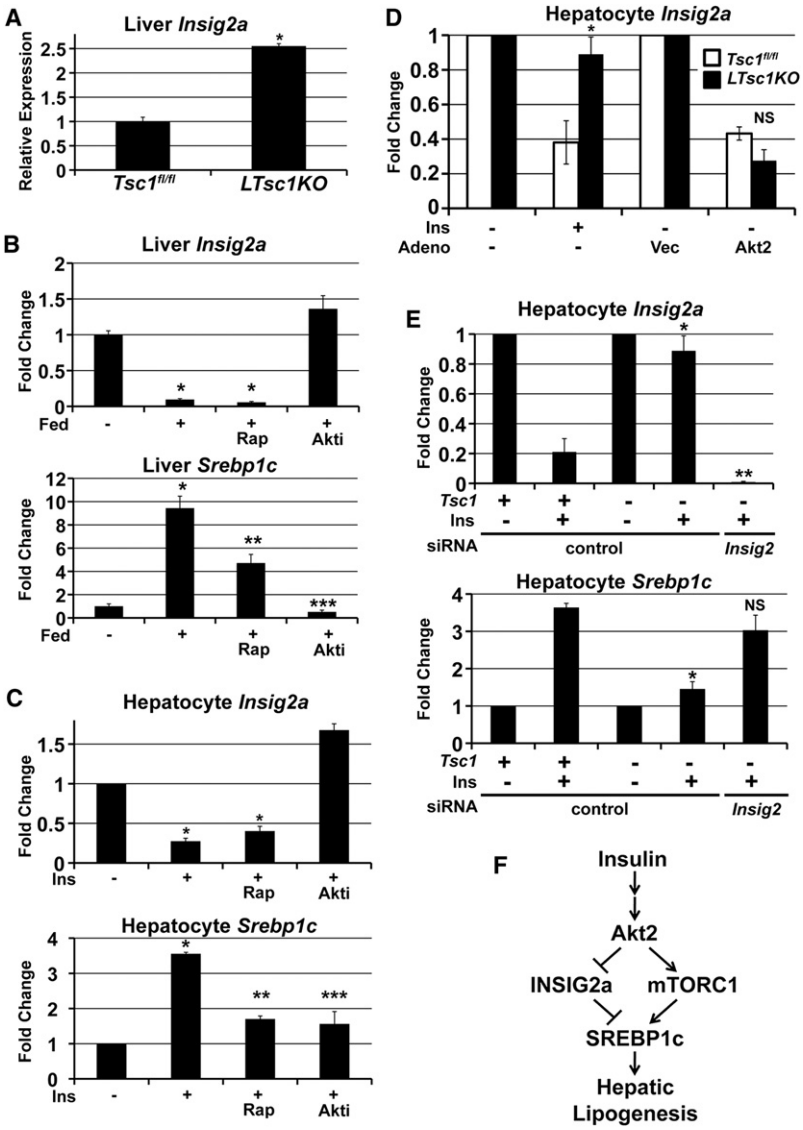

Figure 6. The mTORC1-Independent Pathway to SREBP1c Involves Akt-Mediated Suppression of *Insig2a*

(A) Expression of *Insig2a* in the livers of ad libitum-fed male $Tsc1^{fl/fl}$ (n = 4) and *LTsc1KO* (n = 4) mice on a HFD was measured by qRT-PCR, and levels are presented as mean ± SEM relative to $Tsc1^{fl/fl}$. *p < 0.0002.

(B) Eight-week-old mice were fasted overnight (–) and then refed for 6 hr (+) following a 30 min pretreatment with vehicle, rapamycin (Rap; 10 mg/kg), or Aktviii (Akti; 50 mg/kg) (n = 4 per condition). Hepatic RNA was isolated and gene expression was measured by qRT-PCR. Data are shown as mean ± SEM relative to fasted controls. *p < 3×10^{-6} (*Insig2a*) and p < 0.0002 (*Srebp1c*) compared to fasted; **p < 0.01 and ***p < 0.0008 compared to vehicle-treated fed mice. Note: There is no significant difference between the fold suppression of *Insig2a* by refeeding in the presence or absence of rapamycin or between *Insig2a* levels in fasted mice versus those fed in the presence of Aktviii.

(C) $Tsc1^{fl/fl}$ primary hepatocytes were serum starved overnight and pretreated for 30 min with vehicle, rapamycin (20 nM), or Aktviii (10 μM) prior to 6 hr stimulation with insulin (Ins; 10 nM); gene expression was measured by qRT-PCR. Data are presented as the mean of duplicate samples ± SEM relative to unstimulated cells and are representative of two independent experiments. *Insig2a*: *p < 0.003 for insulin-stimulated suppression and p < 0.01 for insulin-stimulated suppression in the presence of rapamycin. Note: There is no significant difference between the fold suppression of *Insig2a* by insulin in the presence or absence of rapamycin. *Srebp1c*: *p < 0.0003 compared to unstimulated; **p < 0.003 and ***p < 0.03 compared to vehicle-treated, insulin-stimulated samples.

(D) Primary hepatocytes from $Tsc1^{fl/fl}$ and *LTsc1KO* mice were left uninfected or were infected with adenovirus expressing either empty vector (Vec) or myr-Akt2 (Akt2), and 6 hr postinfection, cells were serum starved overnight. Uninfected cells were stimulated with insulin (10 nM) for 6 hr, whereas infected cells were left unstimulated. *Insig2a* expression was measured by qRT-PCR. Data are presented as the mean of duplicate samples ± SEM relative to the unstimulated samples for the uninfected group or the vector-expressing samples for the infected group for each genotype and are representative of at least two independent experiments. *p < 0.05 compared to the fold suppression by insulin in $Tsc1^{fl/fl}$ cells. The fold suppression of *Insig2a* induced by Myr-Akt2 in $Tsc1^{fl/fl}$ and *LTsc1KO* hepatocytes is not significantly different (NS).

(E) $Tsc1^{fl/fl}$ (*Tsc1* +) and *LTsc1KO* (*Tsc1* –) primary hepatocytes were transiently transfected with control or *Insig2* siRNA. Twenty-four hours posttransfection, cells were serum starved overnight, followed by a 6 hr stimulation with insulin (10 nM). Gene expression was measured by qRT-PCR, and levels are presented as the mean of duplicate samples ± SEM relative to unstimulated controls for each genotype. *p < 0.04 (*Insig2a*) and *p < 0.01 (*Srebp1c*) compared to the fold change in response to insulin in $Tsc1^{fl/fl}$ hepatocytes treated with control siRNAs. The insulin-stimulated induction of *Srebp1c* in control siRNA-treated $Tsc1^{fl/fl}$ and *Insig2* siRNA-treated *LTsc1KO* hepatocytes is not significantly different (NS).

(F) Model of two parallel pathways downstream of insulin and Akt2 required for the induction of hepatic SREBP1c and lipogenesis.

et al., 2006; Raghow et al., 2008). SREBP induces the expression of *Insig1*, and the INSIG1 protein is stabilized under sterol-rich conditions, creating an autoinhibitory feedback mechanism (Gong et al., 2006; Horton et al., 2003; Yang et al., 2002). In contrast to INSIG1, the *Insig2* gene is not transcriptionally regulated by SREBP, and the INSIG2 protein is much more stable and unaffected by sterols. Importantly, the predominant liver-specific transcript encoding INSIG2, referred to as *Insig2a*, is strongly downregulated at the message level by insulin signaling (Yabe et al., 2003), perhaps facilitating SREBP1c release from the ER and its subsequent processing and activation. In this study, we find that Akt is responsible for *Insig2a* suppression by insulin and that this occurs independent of mTORC1 signaling. While the pathway by which Akt suppresses *Insig2a* is currently unknown, our data indicate that this is a major mTORC1-independent pathway downstream of Akt in the liver, regulating SREBP1c activation. We hypothesize that the failure to suppress *Insig2a* in *LTsc1KO* hepatocytes blocks the pathway to SREBP1c activation at a step prior to that dependent on mTORC1 signaling. Therefore, insulin induces SREBP1c processing and activation through Akt-mediated suppression of *Insig2a* and stimulation of mTORC1 signaling, which both regulate essential but distinct steps in the pathway to full activation of SREBP1c. Future mechanistic studies are needed to define

both the signaling pathway by which Akt suppresses *Insig2a* expression and the molecular target of mTORC1 signaling involved in promoting SREBP1c activation.

EXPERIMENTAL PROCEDURES

Primary Hepatocyte Cultures

Primary hepatocytes were isolated from 7- to 9-week-old male mice following portal vein collagenase perfusion (Blenzyme 3; Roche) and Percoll gradient purification. For insulin stimulation experiments, hepatocyte cultures were treated as described elsewhere (Li et al., 2010). Infection with adenovirus (Vector Biolabs) was performed 2 hr after plating at an moi of 10. After 6 hr infection, cells were washed once with PBS before serum starving overnight prior to insulin stimulation. Nontargeting control and *Insig2* siRNAs (ON-TARGETplus, Dharmacon) were transiently transfected into primary hepatocytes 6 hr after plating using Lipofectamine 2000 (Invitrogen). Twenty-four hours posttransfection, cells were serum starved overnight prior to insulin stimulation.

Measurement of De Novo Lipogenesis

For the measurement of lipogenesis, primary hepatocytes were cultured and treated as described above. For the final 4 hr of a 6 hr insulin stimulation, cells were labeled with 1-^{14}C acetic acid (Perkin Elmer). Cells were washed twice with PBS before lysis in 0.5% Triton X-100. The lipid fraction was extracted by the addition of chloroform and methanol (2:1 v/v) with vortexing, followed by the addition of water with vortexing. Samples were centrifuged (1000 rpm, 15 min), and ^{14}C incorporation was measured in the bottom, lipid-containing phase using a Beckman LS6500 scintillation counter. Each condition was assayed in duplicate and normalized to protein concentrations in the original lysates.

Gene Expression Analysis

For gene expression analyses, RNA was isolated from mouse tissue using TRIzol (Invitrogen) and from primary hepatocytes using the RNeasy Mini Kit (QIAGEN) and was reverse transcribed into cDNA using the Superscript III First-Strand Synthesis System for RT-PCR kit (Invitrogen). SYBR Green-based quantitative RT-PCR was performed using an Applied Biosystems 7300 Real-Time PCR System. Duplicate or triplicate samples were collected for each experimental condition, and triplicate runs of each sample were normalized to Rplp0 (m36b4) mRNA to determine relative expression levels. The sequences for the primer pairs used in this study are listed in Table S1.

Immunoblotting and Immunohistochemistry

Lysates from cultured primary hepatocytes were prepared as previously described (Manning et al., 2002). Tissue lysates were prepared from tissue that was frozen in liquid nitrogen immediately following resection. Frozen tissue samples were homogenized in NP-40 lysis buffer, and remaining debris was cleared from lysates by subsequent 10 and 30 min spins at 16,000 × *g*. All primary antibodies were obtained from Cell Signaling Technology, except those to tubulin and actin (Sigma) and histone H1, SREBP1, INSIG1, and INSIG2 (Santa Cruz). For immunohistochemistry, paraffin-embedded sections were stained with phospho-S6 (S240/244) using a tissue staining kit (R&D Biosystems).

Mouse Studies

Mice harboring the *Tsc1^{fl}* allele on an FVB background were described previously (Kwiatkowski et al., 2002). For the current study, these mice were crossed onto a C57BL/6J background through seven backcrosses. *Alb-Cre* transgenic mice on this same background were described previously (Postic and Magnuson, 2000). Study cohorts were generated by crossing *Tsc1$^{fl/fl}$* mice with *Alb-Cre Tsc1$^{fl/+}$* mice. PCR genotyping for *Tsc1* and *Cre* was performed as described (Kwiatkowski et al., 2002). Mice were fed either a normal chow diet (9% kcal from fat) or a HFD (60% kcal from fat; F3282, Bio-serv). For fasting-refeeding studies, mice were fasted overnight and either euthanized or refed normal chow for 6 hr. Vehicle (5% Tween-80, 5% PEG-400 in 1× PBS), rapamycin (10 mg/kg), or Aktviii (50 mg/kg; EMD) was administered via i.p. injection 30 min prior to refeeding. Histological preparation and analyses were performed in the Dana-Farber/Harvard Cancer Center Rodent Histopathology Core by R.T. Bronson, an expert rodent pathologist. Liver TGs were measured by enzymatic assay using a kit and were normalized to protein content. Body fat percentage was measured by DEXA (PIXImus).

Statistical Analyses

Statistical significance was measured using a Student's two-tailed t test and a statistical cutoff of $p < 0.05$. Data are presented as mean ± SEM. Immunoblot quantification was performed using ImageJ software.

SUPPLEMENTAL INFORMATION

Supplemental Information includes five figures, one table, and Supplemental Experimental Procedures and can be found with this article online at doi:10.1016/j.cmet.2011.06.002.

ACKNOWLEDGMENTS

We thank R.T. Bronson for histopathological analyses; J.H. Howell and D.E. Cohen for helpful discussions and critical comments regarding this study; and M. Matsuzaki, B. Boback, and J. Nicholatos for technical assistance. This work was supported in part by an NIH training grant (CA009078 to J.L.Y.) and research grants from the American Diabetes Association (1-10-BS-115 to B.D.M.) and the NIH: CA120964 (D.J.K. and B.D.M.), DK52539 and DK64360 (G.S.H.), DK075046 (C.-H.L.), and CA122617 (B.D.M.).

Received: January 28, 2011
Revised: April 29, 2011
Accepted: June 9, 2011
Published: July 5, 2011

REFERENCES

Brown, M.S., and Goldstein, J.L. (2008). Selective versus total insulin resistance: a pathogenic paradox. Cell Metab. *7*, 95–96.

Cho, H., Mu, J., Kim, J.K., Thorvaldsen, J.L., Chu, Q., Crenshaw, E.B., 3rd, Kaestner, K.H., Bartolomei, M.S., Shulman, G.I., and Birnbaum, M.J. (2001). Insulin resistance and a diabetes mellitus-like syndrome in mice lacking the protein kinase Akt2 (PKB beta). Science *292*, 1728–1731.

Cross, D.A., Alessi, D.R., Cohen, P., Andjelkovich, M., and Hemmings, B.A. (1995). Inhibition of glycogen synthase kinase-3 by insulin mediated by protein kinase B. Nature *378*, 785–789.

Cunningham, J.T., Rodgers, J.T., Arlow, D.H., Vazquez, F., Mootha, V.K., and Puigserver, P. (2007). mTOR controls mitochondrial oxidative function through a YY1-PGC-1alpha transcriptional complex. Nature *450*, 736–740.

Dibble, C.C., Asara, J.M., and Manning, B.D. (2009). Characterization of Rictor phosphorylation sites reveals direct regulation of mTOR complex 2 by S6K1. Mol. Cell. Biol. *29*, 5657–5670.

Düvel, K., Yecies, J.L., Menon, S., Raman, P., Lipovsky, A.I., Souza, A.L., Triantafellow, E., Ma, Q., Gorski, R., Cleaver, S., et al. (2010). Activation of a metabolic gene regulatory network downstream of mTOR complex 1. Mol. Cell *39*, 171–183.

Eldar-Finkelman, H., Seger, R., Vandenheede, J.R., and Krebs, E.G. (1995). Inactivation of glycogen synthase kinase-3 by epidermal growth factor is mediated by mitogen-activated protein kinase/p90 ribosomal protein S6 kinase signaling pathway in NIH/3T3 cells. J. Biol. Chem. *270*, 987–990.

Engelking, L.J., Kuriyama, H., Hammer, R.E., Horton, J.D., Brown, M.S., Goldstein, J.L., and Liang, G. (2004). Overexpression of Insig-1 in the livers of transgenic mice inhibits SREBP processing and reduces insulin-stimulated lipogenesis. J. Clin. Invest. *113*, 1168–1175.

Engelking, L.J., Liang, G., Hammer, R.E., Takaishi, K., Kuriyama, H., Evers, B.M., Li, W.P., Horton, J.D., Goldstein, J.L., and Brown, M.S. (2005). Schoenheimer effect explained—feedback regulation of cholesterol synthesis in mice mediated by Insig proteins. J. Clin. Invest. *115*, 2489–2498.

Fang, X., Yu, S., Tanyi, J.L., Lu, Y., Woodgett, J.R., and Mills, G.B. (2002). Convergence of multiple signaling cascades at glycogen synthase kinase

3: Edg receptor-mediated phosphorylation and inactivation by lysophosphatidic acid through a protein kinase C-dependent intracellular pathway. Mol. Cell. Biol. *22*, 2099–2110.

Fleischmann, M., and Iynedjian, P.B. (2000). Regulation of sterol regulatory-element binding protein 1 gene expression in liver: role of insulin and protein kinase B/cAkt. Biochem. J. *349*, 13–17.

Garofalo, R.S., Orena, S.J., Rafidi, K., Torchia, A.J., Stock, J.L., Hildebrandt, A.L., Coskran, T., Black, S.C., Brees, D.J., Wicks, J.R., et al. (2003). Severe diabetes, age-dependent loss of adipose tissue, and mild growth deficiency in mice lacking Akt2/PKB beta. J. Clin. Invest. *112*, 197–208.

Goldstein, J.L., DeBose-Boyd, R.A., and Brown, M.S. (2006). Protein sensors for membrane sterols. Cell *124*, 35–46.

Gong, Y., Lee, J.N., Lee, P.C., Goldstein, J.L., Brown, M.S., and Ye, J. (2006). Sterol-regulated ubiquitination and degradation of Insig-1 creates a convergent mechanism for feedback control of cholesterol synthesis and uptake. Cell Metab. *3*, 15–24.

Gross, D.N., Wan, M., and Birnbaum, M.J. (2009). The role of FOXO in the regulation of metabolism. Curr. Diab. Rep. *9*, 208–214.

Harrington, L.S., Findlay, G.M., and Lamb, R.F. (2005). Restraining PI3K: mTOR signalling goes back to the membrane. Trends Biochem. Sci. *30*, 35–42.

He, L., Hou, X., Kanel, G., Zeng, N., Galicia, V., Wang, Y., Yang, J., Wu, H., Birnbaum, M.J., and Stiles, B.L. (2010). The critical role of AKT2 in hepatic steatosis induced by PTEN loss. Am. J. Pathol. *176*, 2302–2308.

Hegarty, B.D., Bobard, A., Hainault, I., Ferré, P., Bossard, P., and Foufelle, F. (2005). Distinct roles of insulin and liver X receptor in the induction and cleavage of sterol regulatory element-binding protein-1c. Proc. Natl. Acad. Sci. USA *102*, 791–796.

Horton, J.D., Bashmakov, Y., Shimomura, I., and Shimano, H. (1998). Regulation of sterol regulatory element binding proteins in livers of fasted and refed mice. Proc. Natl. Acad. Sci. USA *95*, 5987–5992.

Horton, J.D., Goldstein, J.L., and Brown, M.S. (2002). SREBPs: activators of the complete program of cholesterol and fatty acid synthesis in the liver. J. Clin. Invest. *109*, 1125–1131.

Horton, J.D., Shah, N.A., Warrington, J.A., Anderson, N.N., Park, S.W., Brown, M.S., and Goldstein, J.L. (2003). Combined analysis of oligonucleotide microarray data from transgenic and knockout mice identifies direct SREBP target genes. Proc. Natl. Acad. Sci. USA *100*, 12027–12032.

Howell, J.J., and Manning, B.D. (2011). mTOR couples cellular nutrient sensing to organismal metabolic homeostasis. Trends Endocrinol. Metab. *22*, 94–102.

Huang, J., and Manning, B.D. (2009). A complex interplay between Akt, TSC2 and the two mTOR complexes. Biochem. Soc. Trans. *37*, 217–222.

Khamzina, L., Veilleux, A., Bergeron, S., and Marette, A. (2005). Increased activation of the mammalian target of rapamycin pathway in liver and skeletal muscle of obese rats: possible involvement in obesity-linked insulin resistance. Endocrinology *146*, 1473–1481.

Koketsu, Y., Sakoda, H., Fujishiro, M., Kushiyama, A., Fukushima, Y., Ono, H., Anai, M., Kikuchi, T., Fukuda, T., Kamata, H., et al. (2008). Hepatic overexpression of a dominant negative form of raptor enhances Akt phosphorylation and restores insulin sensitivity in K/KAy mice. Am. J. Physiol. Endocrinol. Metab. *294*, E719–E725.

Krycer, J.R., Sharpe, L.J., Luu, W., and Brown, A.J. (2010). The Akt-SREBP nexus: cell signaling meets lipid metabolism. Trends Endocrinol. Metab. *21*, 268–276.

Kwiatkowski, D.J., Zhang, H., Bandura, J.L., Heiberger, K.M., Glogauer, M., el-Hashemite, N., and Onda, H. (2002). A mouse model of TSC1 reveals sex-dependent lethality from liver hemangiomas, and up-regulation of p70S6 kinase activity in Tsc1 null cells. Hum. Mol. Genet. *11*, 525–534.

Leavens, K.F., Easton, R.M., Shulman, G.I., Previs, S.F., and Birnbaum, M.J. (2009). Akt2 is required for hepatic lipid accumulation in models of insulin resistance. Cell Metab. *10*, 405–418.

Li, S., Brown, M.S., and Goldstein, J.L. (2010). Bifurcation of insulin signaling pathway in rat liver: mTORC1 required for stimulation of lipogenesis, but not inhibition of gluconeogenesis. Proc. Natl. Acad. Sci. USA *107*, 3441–3446.

Li, Y., Xu, S., Mihaylova, M.M., Zheng, B., Hou, X., Jiang, B., Park, O., Luo, Z., Lefai, E., Shyy, J.Y., et al. (2011). AMPK phosphorylates and inhibits SREBP activity to attenuate hepatic steatosis and atherosclerosis in diet-induced insulin-resistant mice. Cell Metab. *13*, 376–388.

Manning, B.D., Tee, A.R., Logsdon, M.N., Blenis, J., and Cantley, L.C. (2002). Identification of the tuberous sclerosis complex-2 tumor suppressor gene product tuberin as a target of the phosphoinositide 3-kinase/akt pathway. Mol. Cell *10*, 151–162.

Matsumoto, M., Ogawa, W., Akimoto, K., Inoue, H., Miyake, K., Furukawa, K., Hayashi, Y., Iguchi, H., Matsuki, Y., Hiramatsu, R., et al. (2003). PKClambda in liver mediates insulin-induced SREBP-1c expression and determines both hepatic lipid content and overall insulin sensitivity. J. Clin. Invest. *112*, 935–944.

Mordier, S., and Iynedjian, P.B. (2007). Activation of mammalian target of rapamycin complex 1 and insulin resistance induced by palmitate in hepatocytes. Biochem. Biophys. Res. Commun. *362*, 206–211.

Ono, H., Shimano, H., Katagiri, H., Yahagi, N., Sakoda, H., Onishi, Y., Anai, M., Ogihara, T., Fujishiro, M., Viana, A.Y., et al. (2003). Hepatic Akt activation induces marked hypoglycemia, hepatomegaly, and hypertriglyceridemia with sterol regulatory element binding protein involvement. Diabetes *52*, 2905–2913.

Porstmann, T., Santos, C.R., Griffiths, B., Cully, M., Wu, M., Leevers, S., Griffiths, J.R., Chung, Y.L., and Schulze, A. (2008). SREBP activity is regulated by mTORC1 and contributes to Akt-dependent cell growth. Cell Metab. *8*, 224–236.

Postic, C., and Magnuson, M.A. (2000). DNA excision in liver by an albumin-Cre transgene occurs progressively with age. Genesis *26*, 149–150.

Raghow, R., Yellaturu, C., Deng, X., Park, E.A., and Elam, M.B. (2008). SREBPs: the crossroads of physiological and pathological lipid homeostasis. Trends Endocrinol. Metab. *19*, 65–73.

Sengupta, S., Peterson, T.R., Laplante, M., Oh, S., and Sabatini, D.M. (2010). mTORC1 controls fasting-induced ketogenesis and its modulation by ageing. Nature *468*, 1100–1104.

Shimano, H., Horton, J.D., Shimomura, I., Hammer, R.E., Brown, M.S., and Goldstein, J.L. (1997). Isoform 1c of sterol regulatory element binding protein is less active than isoform 1a in livers of transgenic mice and in cultured cells. J. Clin. Invest. *99*, 846–854.

Stiles, B., Wang, Y., Stahl, A., Bassilian, S., Lee, W.P., Kim, Y.J., Sherwin, R., Devaskar, S., Lesche, R., Magnuson, M.A., and Wu, H. (2004). Liver-specific deletion of negative regulator Pten results in fatty liver and insulin hypersensitivity [corrected]. Proc. Natl. Acad. Sci. USA *101*, 2082–2087.

Sundqvist, A., Bengoechea-Alonso, M.T., Ye, X., Lukiyanchuk, V., Jin, J., Harper, J.W., and Ericsson, J. (2005). Control of lipid metabolism by phosphorylation-dependent degradation of the SREBP family of transcription factors by SCF(Fbw7). Cell Metab. *1*, 379–391.

Takaishi, K., Duplomb, L., Wang, M.Y., Li, J., and Unger, R.H. (2004). Hepatic insig-1 or -2 overexpression reduces lipogenesis in obese Zucker diabetic fatty rats and in fasted/refed normal rats. Proc. Natl. Acad. Sci. USA *101*, 7106–7111.

Taniguchi, C.M., Kondo, T., Sajan, M., Luo, J., Bronson, R., Asano, T., Farese, R., Cantley, L.C., and Kahn, C.R. (2006). Divergent regulation of hepatic glucose and lipid metabolism by phosphoinositide 3-kinase via Akt and PKClambda/zeta. Cell Metab. *3*, 343–353.

Um, S.H., Frigerio, F., Watanabe, M., Picard, F., Joaquin, M., Sticker, M., Fumagalli, S., Allegrini, P.R., Kozma, S.C., Auwerx, J., and Thomas, G. (2004). Absence of S6K1 protects against age- and diet-induced obesity while enhancing insulin sensitivity. Nature *431*, 200–205.

Yabe, D., Komuro, R., Liang, G., Goldstein, J.L., and Brown, M.S. (2003). Liver-specific mRNA for Insig-2 down-regulated by insulin: implications for fatty acid synthesis. Proc. Natl. Acad. Sci. USA *100*, 3155–3160.

Yahagi, N., Shimano, H., Hasty, A.H., Matsuzaka, T., Ide, T., Yoshikawa, T., Amemiya-Kudo, M., Tomita, S., Okazaki, H., Tamura, Y., et al. (2002).

Absence of sterol regulatory element-binding protein-1 (SREBP-1) ameliorates fatty livers but not obesity or insulin resistance in Lep(ob)/Lep(ob) mice. J. Biol. Chem. *277*, 19353–19357.

Yang, T., Espenshade, P.J., Wright, M.E., Yabe, D., Gong, Y., Aebersold, R., Goldstein, J.L., and Brown, M.S. (2002). Crucial step in cholesterol homeostasis: sterols promote binding of SCAP to INSIG-1, a membrane protein that facilitates retention of SREBPs in ER. Cell *110*, 489–500.

Yellaturu, C.R., Deng, X., Cagen, L.M., Wilcox, H.G., Park, E.A., Raghow, R., and Elam, M.B. (2005). Posttranslational processing of SREBP-1 in rat hepatocytes is regulated by insulin and cAMP. Biochem. Biophys. Res. Commun. *332*, 174–180.

Yellaturu, C.R., Deng, X., Park, E.A., Raghow, R., and Elam, M.B. (2009). Insulin enhances the biogenesis of nuclear sterol regulatory element-binding protein (SREBP)-1c by posttranscriptional down-regulation of Insig-2A and its dissociation from SREBP cleavage-activating protein (SCAP).SREBP-1c complex. J. Biol. Chem. *284*, 31726–31734.

Zhang, H.H., Lipovsky, A.I., Dibble, C.C., Sahin, M., and Manning, B.D. (2006). S6K1 regulates GSK3 under conditions of mTOR-dependent feedback inhibition of Akt. Mol. Cell *24*, 185–197.